

PLA-Coated Gold Nanoparticles for the Labeling of PLA Biocarriers

Hongjin Qiu, Jutta Rieger, Bernard Gilbert, Robert Jérôme,* and Christine Jérôme

Center for Education and Research on Macromolecules (CERM), University of Liège, Sart-Tilman B6a, B-4000 Liège, Belgium

Received June 20, 2003. Revised Manuscript Received December 5, 2003

Poly-DL-lactide end-capped by a protected thiol was synthesized by bulk ring-opening polymerization (ROP) of DL-lactide initiated by the reaction product of aluminum isopropoxide $[\text{Al}(\text{iOPr})_3]$ with α -(2,4-dinitrophenylsulfenyl) ethanol. After the thiol deprotection, PLA-SH was used to stabilize gold nanoparticles. Either these nanoparticles were prepared in the presence of PLA-SH, or PLA-SH was substituted for part of the undecanethiol (C_{11}SH) that stabilized preformed gold nanoparticles. In contrast to C_{11}SH -coated nanoparticles, those stabilized by PLA-SH were successfully entrapped into 100-nm PLA nanocarriers prepared by nanoprecipitation. This is an easy technique to label PLA biocarriers and therefore trace their fate in vivo.

Introduction

Biocompatibility and biodegradability of polylactides make them well suited to drug delivery¹ and tissue engineering.² Although PLA nanocarriers are suitable for drug delivery, their fate in vivo remains an open question as long as they cannot be directly observed by TEM in histological sections. The labeling of PLA nanocarriers by a “contrasting” agent, such as gold nanoparticles, is thus highly desirable.

Gold nanoparticles are already frequently used as TEM contrast agents (immunogold technique³) in immunocytochemistry. For instance, antibodies adsorbed on gold nanoparticles are routinely used in histology,⁴ which allows for the biospecific labeling of tissues and TEM observations.⁵ Gold-based autometallography⁶ is also a very specific method to detect molecules in biological specimens.

This paper aims at labeling PLA nanocarriers by the direct incorporation of gold nanoparticles, thus on the occasion of PLA nanoprecipitation. PLA nanocarriers

result indeed from the rapid addition of water to a binary solution of PLA and a stabilizing copolymer in DMSO.⁷ The strategy proposed in this work consists of grafting PLA at the surface of gold nanoparticles, which are then dispersed in the DMSO solution of PLA and coprecipitated with formation of gold-labeled PLA nanocarriers. Two methods for the grafting of PLA at the surface of gold nanoparticles have been tested, i.e., the direct formation⁸ of gold nanoparticles in the presence of thiol end-capped poly-DL-lactide (PLA-SH), and the partial substitution, or ligand-exchange,⁹ of the alkylthiol ligands of preformed gold nanoparticles by PLA-SH, which results in a mixed alkyl/PLA stabilizing shell (Scheme 1). Gold nanoparticles have been prepared and stabilized by PLA-SH of different molecular weights according to each technique, and incorporated into PLA nanocarriers by nanoprecipitation.

Experimental Section

Materials. Toluene was dried by refluxing over sodium and distilled under nitrogen before use. dl-Lactide was purchased from Boehringer and purified by recrystallization from a 40 wt % solution in dry toluene. It was dried at room temperature, under reduced pressure, for 24 h before polymerization. Aluminum isopropoxide $[\text{Al}(\text{iOPr})_3]$ was sublimated, and then dissolved in dry toluene (0.25 M) under nitrogen. Lactide was bulk polymerized as reported elsewhere.¹⁰ Mercaptoethanol was dried over anhydrous magnesium sulfate (MgSO_4) and distilled just before use. All the other reagents were used as received: $\text{HAuCl}_4 \cdot x\text{H}_2\text{O}$ (Strem, 99.9%); $\text{N}(\text{C}_8\text{H}_{17})_4\text{Br}$ (Aldrich, 98%); NaBH_4 (Janssen, 98%); and C_{11}SH (Aldrich, 98%).

(7) Gautier, S.; Grudzielski, N.; Goffinet, G.; Hassonville, S. H. D.; Delattre, L.; Jérôme, R. *J. Biomater. Sci. Polym.* **2001**, *12*, 429. Grandfils, C.; Nihant, N.; Jérôme, R.; Teyssié, P. *U.S. Patent* 5,962,566, 1999.

(8) Brust, M.; Walker, M.; Bethell, D.; Schiffrin, D. J.; Whyman, R. *J. Chem. Soc., Chem. Commun.* **1994**, 801.

(9) Hostetler, M. J.; Green, S. J.; Stokes, J. J.; Murray, R. W. *J. Am. Chem. Soc.* **1996**, *118*, 4212.

(10) Degée, P.; Dubois, P.; Jérôme, R. *Macromol. Symp.* **1997**, *123*, 67.

* To whom correspondence should be addressed. E-mail: rjerome@ulg.ac.be.

(1) Kreuter, J. *J. Control. Relat.* **1991**, *16*, 169. Alleman, E.; Gurny, R.; Doelker, E. *Eur. J. Pharm. Biopharm.* **1993**, *39*, 173. Deng, X.; Liu, Y.; Yuan, M.; Li, X.; Lin, L.; Jia, W. X. *J. Appl. Polym. Sci.* **2002**, *86*, 2557.

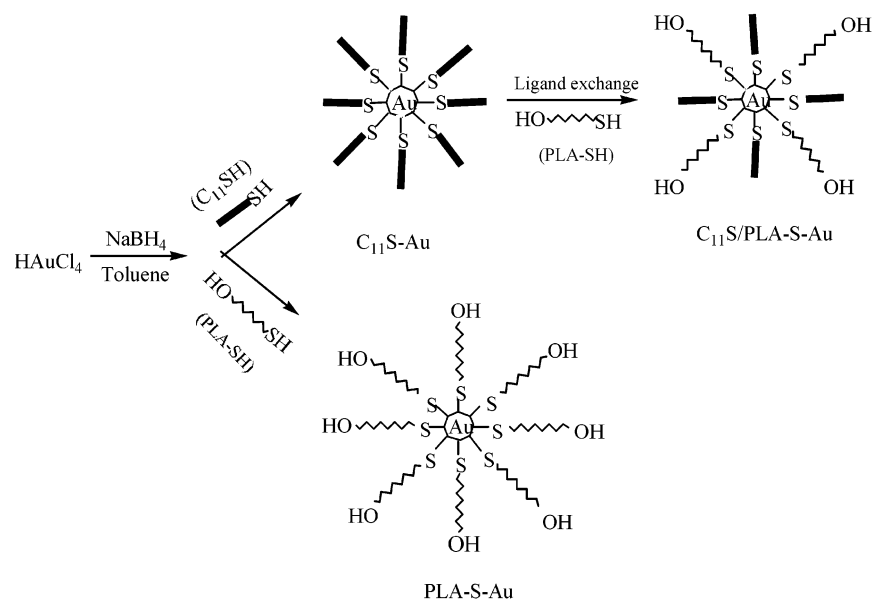
(2) Kulkarni, R. K.; Moore, E. G.; Hegyeli, F.; Leonard, F. *J. Biomed. Mater. Res.* **1971**, *5*, 163. Pitt, C. G.; Marks, T. A.; Schlinder, A. In *Biodegradable Drug Delivery Systems Based on Aliphatic Polyesters: Application of Contraceptives and Narcotic Antagonists, Controlled Release of Bioactive Materials*; Baker, R., Ed.; Academic: New York, 1980.

(3) De Mey, J. *Immunocytochemistry, Practical Application in Pathology and Biology*; Polak, J. M., Van Naarden, S., Eds.; Wright-PSG, Boston, MA, 1983; Chapter 6, p 83.

(4) Kreuter, J. In *Microcapsules and Nanoparticles in Medicine and Pharmacy*; Donbrow, M., Ed.; CRC: Boca Raton, FL, 1992.

(5) Safer, D. E.; Bolinger, L.; Leigh, J. S. *J. Inorg. Biochem.* **1986**, *26*, 77. Safer, D. E.; Hainfeld, J.; Wall, J. S.; Reardon, J. E. *Science* **1982**, *218*, 290. Hainfeld, J. F.; Furuya, F. R. *J. Histochem., Cytochem.* **1992**, *40*, 177.

(6) Weipoltshammer, K.; Schofer, C.; Almeder, M.; Wachtler, F. *Histochem. Cell. Biol.* **2000**, *114*, 489.

Scheme 1. Synthetic Route of Gold Nanoparticles Stabilized by Undecanethiol and/or Polylactide Thiol**Table 1. Characteristic Features of Thiol-Functionalized Polylactide**

polylactide	type	[M ₀]/[Al]	conversion %	M _n ^a		polydispersity (M _w /M _n)
				¹ H NMR	SEC	
PLA1	protected	64	100	3500	3800	2.10
PLA1-SH	deprotected			4700	4800	
PLA2	protected	25	100	1200	800	4.00
PLA2-SH	deprotected			2100	2400	

^a M_n: number average molecular weight.

Synthesis of α-(2,4-Dinitrophenylthio) ethanol (A)¹¹. A solution of 0.39 g of mercaptoethanol (5.0 mmol) in 4.0 mL of CHCl_3 was slowly added to a solution of 0.94 g (5.0 mmol) of 2,4-dinitrofluorobenzene mixed with 1.4 mL of triethylamine (10.0 mmol) in 6.0 mL of chloroform. The reaction mixture was stirred at room temperature for 15 h. It was neutralized with HCl (1.0 M) and then washed twice with water. Yellow crystals were collected from the organic phase and recrystallized from CHCl_3 . Yield (68%).

¹H NMR (CDCl_3): δ 9.06 (s, 1H, -Ar), δ 8.27 (d, 1H, -Ar), δ 7.75 (d, 1H, Ar), δ 4.05 (t, 2H, $-\text{SCH}_2\text{CH}_2\text{OH}$), δ 3.30 (t, 2H, $-\text{SCH}_2\text{CH}_2\text{OH}$).

Synthesis of Poly-DL-lactide End-Capped by a Protected Thiol (PLA-A). The initiator was prepared by reaction of 1 equiv of Al (*i*OPr)₃ with 3 equiv of compound A in toluene. The solvent was distilled off regularly to displace the 2-propanol formed as a byproduct. It was replaced by freshly dried toluene, and the azeotropic distillation was repeated (2 times). DL-Lactide was bulk polymerized at 130 °C, in a previously flamed and nitrogen-purged flask, for 20 h. End-functional poly-DL-lactide (Table 1; entries 1 and 3) was dissolved in THF, precipitated in heptane, and dried in vacuo (yield: 82%).

Deprotection of the Thiol End-Group of PLA-A. PLA end-capped by a protected thiol was dissolved in CHCl_3 in the presence of 1-propanethiol (100 equiv). Triethylamine was added until pH was 8. The reaction mixture was stirred under nitrogen for 15 h. After elimination of the unreacted 1-propanethiol, it was poured in heptane, and the thiol end-capped PLA (PLA-SH) was precipitated (Table 1; entries 2 and 4).

Preparation of Gold Nanoparticles Stabilized by C₁₁SH and PLA-SH. Gold nanoparticles were prepared according to Brust et al.⁸ except for the Au/S molar ratio, which was 3.5:1 as recommended by D. V. Leff et al.¹² In a typical experiment,

25.48 mg of $\text{HAuCl}_4 \cdot x\text{H}_2\text{O}$ was dissolved in 2.46 mL of deionized water. A 1.65-mL aliquot of a $\text{N}(\text{C}_8\text{H}_{17})_4\text{Br}$ solution in toluene (0.10 M) was added to the aqueous solution under rapid stirring ($\text{N}(\text{C}_8\text{H}_{17})_4\text{Br}/\text{Au} = 2.22:1$). The two-phase mixture was vigorously stirred until the tetrachloroaurate was completely transferred to the organic phase, which was then separated from the slightly orange aqueous phase. The organic solution was added with 0.51 mL of a C₁₁SH solution in toluene (0.042 M), followed by the slow addition of 2.0 mL of a freshly prepared aqueous solution (0.41 M) of NaBH_4 ($\text{NaBH}_4/\text{Au} = 11.0:1$) under vigorous stirring for 12 h. The organic phase was separated and concentrated until 1.0 mL was left, and finally added into 75 mL of ethanol (96%). This mixture was kept at -20 °C for 48 h, and the dark brown precipitate was collected by centrifugation and dried in vacuo (Table 2; entry 1). When PLA-SH was used instead of C₁₁SH, the reaction time was 4 h (Table 2; entries 4 and 5).

Ligand Exchange for the Preparation of C₁₁S/PLA-S Stabilized Gold Nanoparticles. The ligand-exchange reaction⁹ was carried out by adding PLA-SH to the C₁₁S-Au dispersion in toluene. In a typical experiment, 4.0 mg of C₁₁S-Au in 2.0 mL of toluene were added to 6.4 mg of PLA-SH ($M_n = 2400$), and stirred for 48 h at room temperature. The solvent was removed in vacuo, and the collected material was washed abundantly with absolute ethanol and recovered by centrifugation (Table 2; entries 2 and 3). The Au/S atomic ratio was 4.2 for the C₁₁S-Au nanoparticles according to the data reported elsewhere.¹²

Characterization. Polylactide was analyzed by ¹H NMR spectroscopy with a Bruker AM 400 apparatus at 25 °C, in deuterated chloroform added with tetramethylsilane as an internal reference. Number-average molecular weight was calculated from the intensity ratio for the CH protons of the lactide units ($\delta = 5.2$) and the CH₂ protons adjacent to the sulfide end-group ($\delta = 3.3$) (Figure 1A). It was also determined by size exclusion chromatography (SEC) in THF with a HP 1090 liquid chromatograph, equipped with a HP 1037 A refractive index detector and four PL GEL columns of various

(11) Trollsas, M.; Hawker, C. J.; Hedrick, J. L. *Macromolecules* **1998**, *31*, 5960.

(12) Leff, D. V.; Ohara, P. C.; Heath, J. R.; Gelbart, W. M. *J. Phys. Chem.* **1995**, *99*, 7036.

Table 2. Dispersions of Gold Nanoparticles in Organic Solvents^a

nanoparticle	solvent					size (nm)
	water	heptane	toluene	chloroform	DMSO	
C11S-Au	—	+	+	+	—	7 ± 2
C11S/PLA1-S-Au	—	—	+	+	+	2 ± 1
C11S/PLA2-S-Au	—	—	+	+	+	3 ± 1
PLA1-S-Au	—	—	—	—	+	6 ± 1
PLA2-S-Au	—	—	—	—	+	5 ± 1

^a +, Dispersible; —, not dispersible; DMSO, dimethyl sulfoxide; 1, PLA1-SH with $M_n = 2400$ and PLA1-S/C11S ratio is 0.4; 2, PLA2-SH with $M_n = 4800$ and PLA2-S/C11S ratio = 0.6. Size was estimated by measuring over 100 nanoparticles on enlarged TEM images.

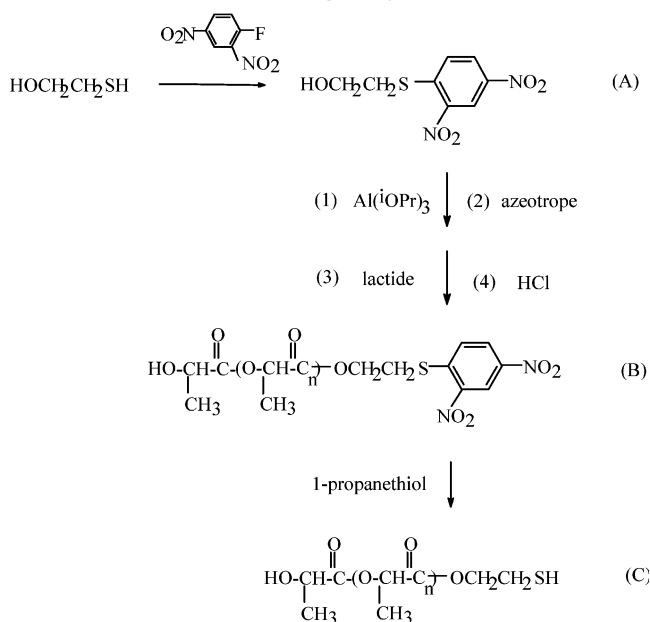
pore sizes (10^5 , 10^4 , 500, and $100 \mu\text{m}$). Absolute molecular weights were calculated by using polystyrene standards and the Mark-Houwink equations for polystyrene ($K_{PS} = 1.25 \times 10^{-4} \text{ dl/g}$, $\alpha_{PS} = 0.707$) and polylactide ($K_{PLA} = 5.49 \times 10^{-4} \text{ dl/g}$ and $\alpha_{PLA} = 0.639$), respectively.

Transmission electron micrographs (TEM) were recorded with a Philips CM-100 microscope. Samples were prepared by spreading a drop of a dilute dispersion of particles on a copper grid coated with Formvar. UV-vis spectra were recorded for gold nanoparticles dispersed in chloroform and DMSO. Raman spectra of gold nanoparticles were recorded with a LabRam spectrometer (Jobin-Yvon) equipped with a confocal microscope and a liquid-N₂ cooled open-electrode CCD. The spectral resolution was 2 cm^{-1} . The excitation laser beam (514.5 nm) was focused on the sample, previously deposited onto a glass plate and dried. To prevent the colored sample from being burnt, the power of the laser was kept at the minimum value (0.5 mW), and the integration time was increased accordingly (100 sec). Because of the grating dispersion and the length of the CCD detector (1 in.), the full spectrum was recorded in two parts, covering the $200\text{--}1800 \text{ cm}^{-1}$ and $2400\text{--}3700 \text{ cm}^{-1}$ ranges, respectively. Dynamic light scattering (DLS) was carried out with a Brookhaven instrument (Ar laser, 488 nm) with a suspension diluted by filtered deionized water until a PLA concentration of $50 \mu\text{g/mL}$ was reached. The size distribution was calculated by the Contin method.

Results and Discussion

1. Poly-DL-lactide End-Capped By Thiols. A few examples of thiol end-capped chains have been reported in the scientific literature.¹³ In this work, a method reported for poly(ϵ -caprolactone) (PCL) by Hedrick et al.¹¹ has been extended to PLA. As shown in Scheme 2, the thiol has been protected by 2,4-dinitrofluorobenzene (Sangers reagent), which is highly reactive toward a variety of functional groups.¹⁴ Deprotection is possible under mild conditions as discussed hereafter. Moreover, the aromatic protecting group can be unambiguously identified by ^1H NMR, which is an advantage for

Scheme 2. Synthetic Route for the Thiol End-Capping Polylactide



monitoring both the end-capping and the deprotection reactions. In this respect, Figure 1A shows the ^1H NMR spectrum for PLA end-capped by the protected thiol. Resonances typical of PLA are observed at 5.16 and 1.56 ppm.^{10,15} The aromatic protons of the 2, 4-dinitrophenylsulfenyl moiety are observed at 9.09, 8.42, and 7.73 ppm. The chemical shifts for the protons of the two methylene groups between the O and S atoms are at 4.43 and 3.33 ppm, respectively, thus different from the values noted for 2,4-dinitrophenylsulfenyl ethanol, i.e., $\delta = 4.05$ and 3.31 ppm. This peaks assignment allows for the molecular weight of PLA to be calculated (intensity ratio of peaks f and d) and compared to SEC data as shown in Table 1. Bulk polymerization of LA at 130°C results in a broad molecular weight distribution ($M_w/M_n = 4.0$ for low M_n (1200) and 2.1 for $M_n = 3500$). A slow initiation compared to propagation, together with the slow dissolution of the initiator in the molten monomer, contribute to this effect.

The thiol end-group of PLA has been deprotected by a large excess of 1-propanethiol in chloroform. This solvent is needed for the deprotection of PLA of the higher M_n (3500) to be quantitative. The ^1H NMR spectrum (Figure 1B) confirms the successful deprotection of PLA. The resonance peaks (a, b, and c) for the phenyl group have disappeared, in contrast to peak d ($-\text{S}-\text{CH}_2-$) which has been shifted significantly from

(13) Stouffer, J. M.; McCarthy, T. J. *Macromolecules* **1988**, *21*, 1204. Premachandran, R.; Banerjee, S.; John, V. T.; McPherson, G. L. *Chem. Mater.* **1997**, *9*, 1342. Hirao, A.; Shione, H.; Wakabayashi, S.; Nakahama, S.; Yamaguchi, K.; *Macromolecules* **1994**, *27*, 1835. Tohyama, M.; Hirao, A.; Nakahama, S.; *Makromol. Chem. Phys.* **1996**, *197*, 3135. Corbierre, M. K.; Cameron, N. S.; Sutton, M.; Mochrie, S. G. J.; Lurio, L. B.; Rühm, A.; Lennox, R. B. *J. Am. Chem. Soc.* **2001**, *123*, 10411. Nuss, S.; Böttcher, H.; Wurm, H.; Hallensleben, M. L. *Angew. Chem., Int. Ed.* **2001**, *40*, 4016. Chiefari, J.; Chong, Y. K.; Ercole, F.; Krstina, J.; Jeffery, J.; Le, T. P. T.; Mayadunne, R. T. A.; Meijs, G. F.; Moad, C. L.; Moad, G.; Rizzardo, E.; Thang, S. H. *Macromolecules* **1998**, *31*, 5559. Sumerlin, B. S.; Donovan, M. S.; Mitsukami, Y.; Lowe, A. B.; McCormick, C. L. *Macromolecules* **2001**, *34*, 6561. Mitsukami, Y.; Donovan, M. S.; Lowe, A. B.; McCormick, C. L. *Macromolecules* **2001**, *34*, 2248. Donovan, M. S.; Lowe, A. B.; Sumerlin, B. S.; McCormick, C. L. *Macromolecules* **2002**, *35*, 4123. Donovan, M. S.; Sanford, T.; Lowe, A. B.; Mitsukami, Y.; Sumerlin, B. S.; McCormick, C. L. *Macromolecules* **2002**, *35*, 4570.

(14) Sanger, F. *Biochem. J.* **1945**, *39*, 507. Zahn, H.; Trautmann, K. Z. *Naturforsch.* **1954**, *9B*, 578. Siepmann, E.; Zahn, H. *Biochim. Biophys. Acta* **1964**, *82*, 412. Prisco, G. D. *Biochem. Biophys. Res. Commun.* **1967**, *26*, 148. Shaltiel, S. *Biochem. Biophys. Res. Commun.* **1967**, *29*, 178.

(15) Degée, P.; Dubois, P.; Jérôme, R. *Macromol. Chem. Phys.* **1997**, *198*, 1973.

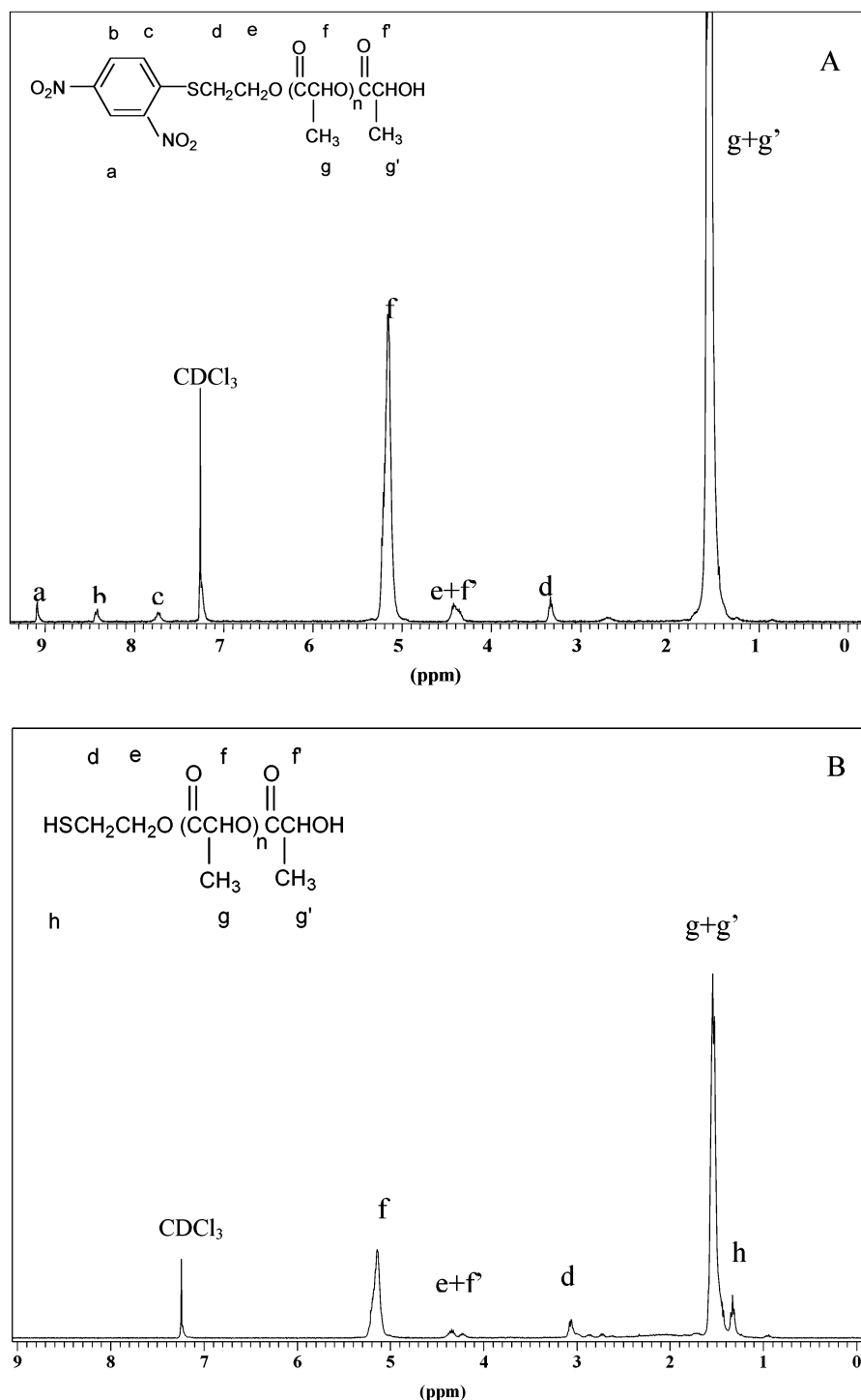


Figure 1. ^1H NMR spectra for thiol end-capped polylactide: (A) before, (B) after deprotection.

$\delta = 3.33$ to $\delta = 3.10$ ppm. Consistently, an additional peak assigned to $-\text{SH}$ is observed at $\delta = 1.32$ ppm. Unexpectedly, M_n of PLA is higher and the polydispersity is lower after deprotection. The only reasonable explanation is that the shorter chains are lost when PLA is purified by reprecipitation in heptane. More PLA is recovered when it is precipitated at low temperature rather than at room temperature, which confirms that the PLA solubility is very sensitive to molecular weight at least in the temperature range under consideration.

Gold Nanoparticles Stabilized by Thiol End-Capped PLA. $\text{C}_{11}\text{S}-\text{Au}$ nanoparticles have been prepared by an in-situ method⁸ and used as a reference to

investigate whether PLA-SH can have a beneficial effect on the stability of dispersion of gold nanoparticles in various solvents. These particles are waxy with a dark-brown color. They are repeatedly dispersible in nonpolar or weakly polar solvents, such as heptane, toluene, and chloroform, but not at all in more polar solvents, such as DMSO (Table 2). PLA-SH has then been exchanged for the ligand of the $\text{C}_{11}\text{S}-\text{Au}$ nanoparticles (Scheme 1), according to two PLA-S/ C_{11}S ratios, i.e., 0.4 and 0.6, respectively. The particles then appear as a solid with a light brown color. They are dispersible in toluene, chloroform, and highly polar DMSO, but no longer in heptane which is a nonsolvent for PLA (Table 2). This

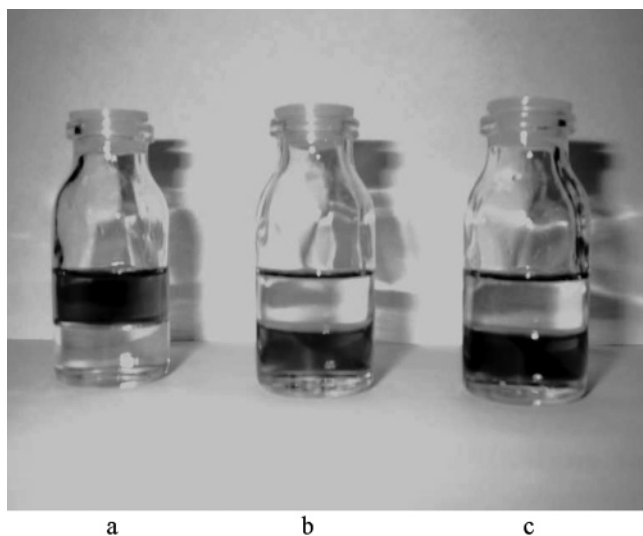


Figure 2. Dispersion of gold nanoparticles in two-phase heptane (top)/DMSO (bottom) mixtures. Stabilization by (a) undecanethiol, (b) mixed undecanethiol/poly lactide-thiols, and (c) polylactide-thiol.

observation is valid to the set of PLA chains listed in Table 1. Whenever PLA-S-Au nanoparticles are prepared in a direct way (in-situ method; Scheme 2), Table 2 shows that they can be redispersed after purification only in DMSO with a deep purple color. These gold nanoparticles have been dispersed in two-phase heptane/DMSO mixtures as illustrated in Figure 2. These observations indicate that the dispersion stability closely depends on the amount of PLA-SH adsorbed onto the gold nanoparticles. Indeed, stability is noted in solvents

of increasing polarity (heptane < toluene and chloroform < DMSO) when the undecanethiol ligand ($C_{11}SH$) is replaced partly (29% and 38%, as confirmed by 1H NMR) and then completely by PLA-SH.

Gold nanoparticles have been observed by transmission electron microscopy (TEM). Figure 3 shows spherical nanoparticles, the sizes of which are reported in Table 2. Nanoparticles with a corona of mixed ligands ($C_{11}S$ and PLA-S) are significantly smaller (Figure 3c and d) than the $C_{11}S$ -Au coated particles (Figure 3a) with a more uniform size distribution. This modification is typical for particles prepared by the ligand-exchange method,¹⁶ more likely because they are recovered by centrifugation after reaction. The non- (or not extensively enough) modified $C_{11}S$ -Au nanoparticles would not precipitate in the excess of ethanol, so leading to size fractionation. Although the difference is not very important ($\pm 15\%$), the PLA1-S-Au nanoparticles are smaller than the $C_{11}S$ -Au ones, which could be reasonably explained by a simple molecular packing model as shown in Figure 4. The solvated PLA chains are supposed to be coiled, compared to the short C_{11} alkyl radicals, which would be rather rod-shaped.¹⁷ Therefore, the PLA chains are less densely packed at the gold surface, with the consequence that the occupied area is larger, and the gold nanoparticles are smaller. The space conformation of the ligand can thus affect the size of the stabilized gold nanoparticles.¹⁸

UV-vis spectroscopy was used to characterize the gold nanoparticles (Figure 5). The maximum of absorption, which corresponds to the gold plasmon resonance,¹⁹ is known to depend on several factors including particle

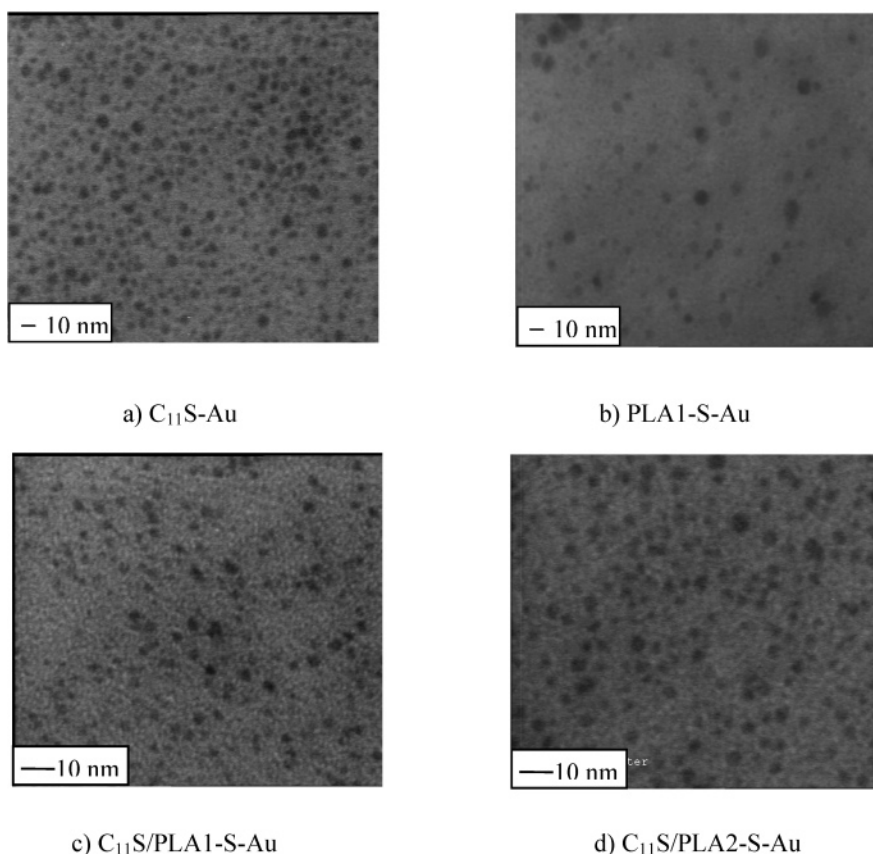


Figure 3. TEM of gold nanoparticles stabilized by (a) undecanethiol, (b) polylactide-thiol, (c) undecanethiol/poly lactide (M_n 2400) thiol, and (d) mixed undecanethiol/poly lactide (M_n 4800) thiols.

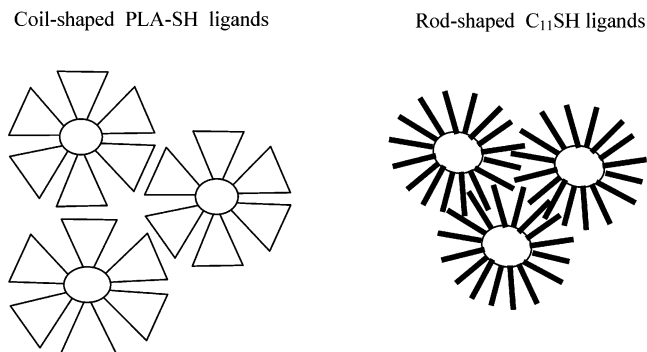


Figure 4. Molecular packing model for gold nanoparticles stabilized by PLA-SH and C₁₁SH.

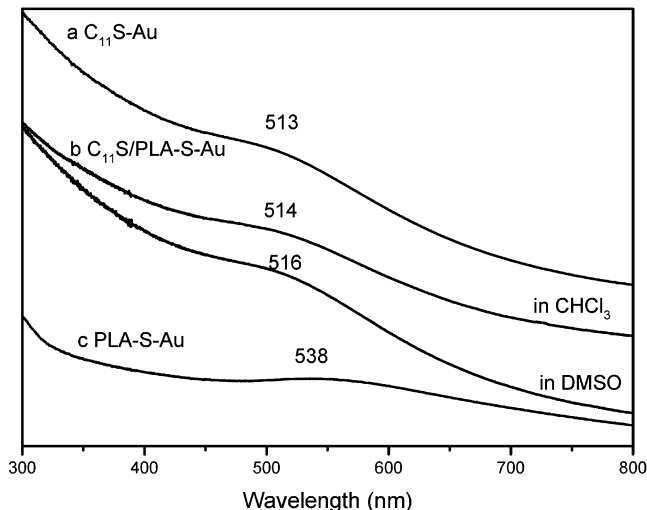


Figure 5. UV-vis spectra for thiol-stabilized gold nanoparticles in different solvents at room temperature: (a) undecanethiol (CHCl₃), (b) undecanethiol/poly(lactide (M_n 2400) thiol (CHCl₃ and DMSO), and (c) polylactide (M_n 2400) thiol (DMSO).

size, surface functionality, solvent, and temperature.²⁰ No significant modification is observed in the maximum absorption for the C₁₁S-Au and C₁₁S/PLA-S-Au particles, whereas a bathochromic shift is observed for the PLA-S-Au ones. This shift cannot be accounted for by a solvent effect (comparison of CHCl₃ and DMSO in Figure 5b), and it is exceedingly large for being explained by the difference in the particles' size reported in Table 2. A possible explanation might be found in the way that the ligands (C₁₁S-Au and PLA-S) interact with the gold surface. Although the C₁₁ alkyl substituents have no reason to interact with the metal, this is not the case for the ester of the PLA monomer units (Figure 5a and c). However, when the two types of ligands coexist (Figure 5b), only the chemisorption of the thiol would be effective.

(16) Brown, L. O.; Hutchison, J. E. *J. Am. Chem. Soc.* **1999**, *121*, 882. Martin, J. E.; Wilcoxon, J. P.; Odinek, J.; Provencio, P. *J. Phys. Chem. B* **2000**, *104*, 9475.

(17) Ullman, A. *Chem. Rev.* **1996**, *96*, 1533. Yonezawa, T.; Onoue, S.; Kunitake, T. *Polym. Prepr. Jpn.* **1999**, *48*, 3547.

(18) Yonezawa, T.; Yasui, K.; Kimizuka, N. *Langmuir* **2001**, *17*, 271.

(19) Henglein, A. *J. Phys. Chem.* **1993**, *97*, 5457.

(20) Hostetler, M. J.; Wingate, J. E.; Zhong, C. J.; Harris, J. E.; Vachet, R. W.; Clark, M. R.; Londono, J. D.; Green, S. J.; Stokes, J. J.; Wignall, G. D.; Glish, G. L.; Porter, M. D.; Evans, N. D.; Murray, R. W. *Langmuir* **1998**, *14*, 17. Link, S.; El-Sayed, M. A. *J. Phys. Chem. B* **1999**, *103*, 4212. Shipway, A. N.; Katz, E.; Willner, I. *ChemPhysChem* **2000**, *1*, 18.

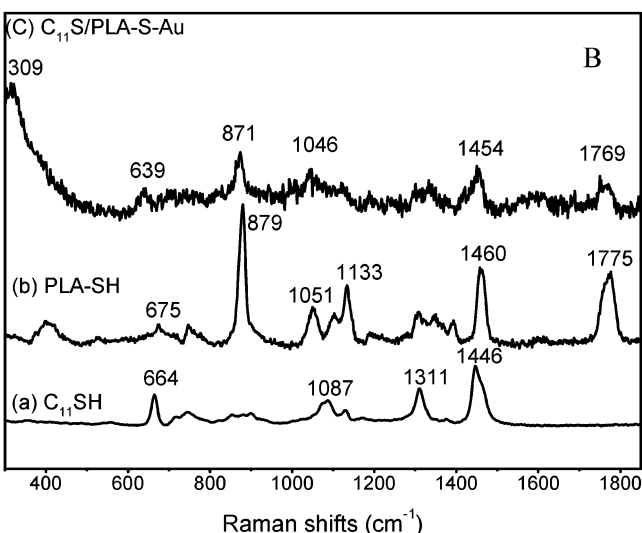
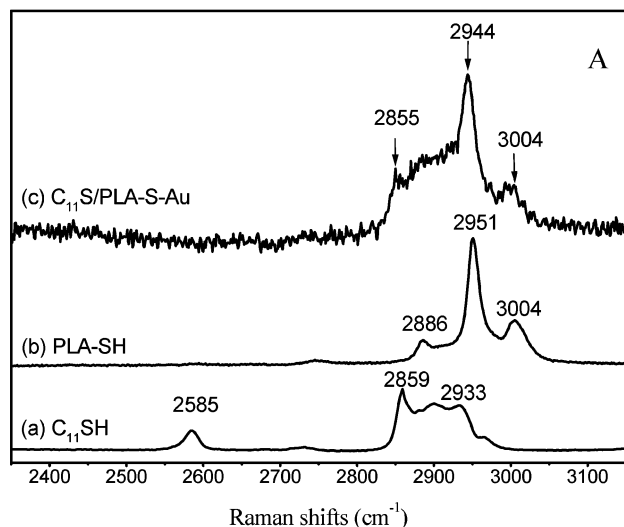


Figure 6. Raman spectra in the 2350–3150 cm⁻¹ region (6A) and in the 300–1850 cm⁻¹ region (6B), for liquid undecanethiol (A), solid polylactide thiol (B), and gold nanoparticles stabilized by undecanethiol/poly(lactide (M_n 2400) thiol (c).

Thiol-stabilized nanoparticles have been characterized by Raman spectroscopy in the scientific literature.²¹ In this study, Raman spectra have been recorded to confirm that the ligand exchange of PLA-SH for C₁₁SH is efficient. Figure 6 shows bands characteristic of the C–H binding at 2859–2933 cm⁻¹ for (unadsorbed) C₁₁SH (Figure 6A-a), and at 2886 and 2951 cm⁻¹ for (unadsorbed) PLA-SH (Figure 6A-b). The bands of C₁₁S and PLA-S remain visible in the case of the C₁₁S/PLA-S-Au nanoparticles (Figure 6A-c). Moreover, the band assigned to S–H of C₁₁SH at 2585 cm⁻¹ is no longer observed for the C₁₁S/PLA-S-Au nanoparticles, in agreement with the formation of a S–Au bonding. Figure 6 B shows the C–S stretching region, which provides structural information on the fragment adjacent to the sulfur headgroup.²² The band at 639 cm⁻¹ is typical of the C–S bonding,²² when S is linked to gold in the C₁₁S/PLA-S-Au nanoparticles. The Raman spec-

(21) Lee, P. C.; Meisel, D. *J. Phys. Chem.* **1982**, *86*, 3391. Xu, H.; Tseng, C. H.; Vickers, T. J.; Mann, C. K.; Schlenoff, J. B. *Surf. Sci.* **1994**, *311*, L707.

(22) Hostetler, M. J.; Stokes, J. J.; Murray, R. W. *Langmuir* **1996**, *12*, 3604.

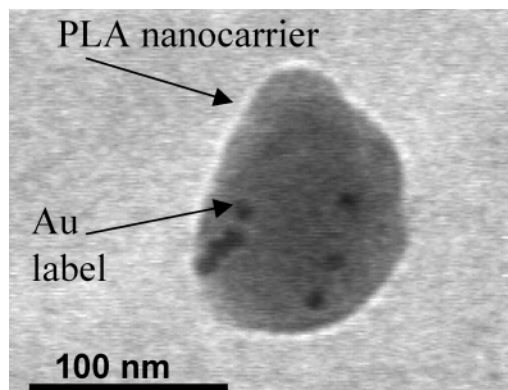


Figure 7. TEM of polylactide nanocarriers labeled by $C_{11}S/PLA-S-Au$ nanoparticles (M_n of PLA 2400).

trum for the $C_{11}S/PLA-S-Au$ nanoparticles also shows bands at 1769 cm^{-1} characteristic of the PLA ester groups and at 1454 , 1046 , and 871 cm^{-1} , which confirms the contribution of PLA-SH to the stabilization of the gold nanoparticles. Moreover, the Au-S bonding is observed at 309 cm^{-1} , which confirms that the nanoparticles are stabilized by thiols.

Labeling of PLA Nanocarriers. The gold nanoparticles stabilized by the mixed $C_{11}SH/PLA-SH$ shell have been successfully dispersed in DMSO, without alteration of size or shape, thus without aggregation. They have been encapsulated in polylactide nanocarriers prepared by nanoprecipitation as reported by S. Gautier et al.⁷ (Figure 7). Briefly, the PLA nanocarriers were prepared by rapid addition of water (4-fold excess) to a DMSO solution of poly-DL-lactide (16 mg/mL; M_n 50000) and poly(methyl methacrylate-*co*-methacrylic acid) (PMMA-*co*-MA) (1.6 mg/mL; M_n = 13 000, MA content = 25 mol %). The average size of the accordingly formed PLA nanocarriers is ca. 100 nm.

Labeling of PLA nanocarriers by addition of conventional negatively charged Au-citrate nanoparticles²³ or commercially available (Sigma) hydrophilic Au-streptavidin nanoparticles to the aqueous phase used to (nano)-precipitate PLA was not successful. Indeed, a weak affinity for PLA and a highly stable dispersion in water

prevent these hydrophilic gold nanoparticles from coprecipitating with PLA. In contrast, when $C_{11}S/PLA-S-Au$ (ca. 2.44 nm) or $PLA-S-Au$ (ca. 5.56 nm) nanoparticles are dispersed in the DMSO solution, they are successfully encapsulated in the PLA nanocarriers (Figure 7). DLS measurements have shown that the size ($136 \pm 12\text{ nm}$) and size distribution of the PLA nanocarriers are not significantly modified by the gold nanoparticles. Moreover, the gold-labeled nanocarriers do not exhibit higher propensity to aggregation than the neat nanoparticles in solution. The PLA-S- shell makes gold nanoparticles appropriate to the labeling of PLA nanocarriers and their tracing within tissues. In vivo experiments are under current investigation.

Conclusion

Thiol end-capped PLA has been synthesized by ROP of lactide initiated by a protected thiol containing alcohol, followed by deprotection. The efficiency of the end-capping and deprotection reactions has been confirmed by 1H NMR. After deprotection of the thiol end-group, M_n is increased and the polydispersity is decreased, as a result of fractionation when the thiol end-capped PLA is reprecipitated in heptane. Gold nanoparticles have been successfully stabilized by PLA-SH, either directly by the in situ method in a two-phase system or by a ligand-exchange reaction. Stability of dispersions of PLA-SH coated gold nanoparticles in DMSO increases with the amount of PLA-SH attached to the surface ($PLA-S-Au > C_{11}S/PLA-S-Au > C_{11}S-Au$). TEM shows that the average size lies in the range 7–2 nm depending on the structure and size of the ligand(s). These $C_{11}S/PLA-S-Au$ and $PLA-S-Au$ nanoparticles can be successfully encapsulated in PLA nanocarriers, which are accordingly labeled and could be traced by autometallography of TEM sections.⁶

Acknowledgment. We are much indebted to the Services Fédéraux des Affaires Scientifiques, Techniques et Culturelles for general support in the frame of the Pôles d'Attraction Universitaires PAI V/03. C.-J. is Chercheur Qualifié by the Fonds National de la Recherche Scientifique.

CM034519G

(23) Jana, N. R.; Gearheart, L.; Murphy, C. J. *Langmuir* **2001**, *17*, 6782.